A Novel Mammalian Myosin I from Rat with an SH3 Domain Localizes to Con A–Inducible, F-Actin–rich Structures at Cell–Cell Contacts

Hanns-Eugen Stöffler, Christian Ruppert, Jutta Reinhard, and Martin Bähler

Friedrich-Miescher-Laboratorium der Max-Planck-Gesellschaft, D-72076 Tübingen, Germany

Abstract. In an effort to determine diversity and function of mammalian myosin I molecules, we report here the cloning and characterization of myr 3 (third unconventional myosin from rat), a novel mammalian myosin I from rat tissues that is related to myosin I molecules from protozoa. Like the protozoan myosin I molecules, myr 3 consists of a myosin head domain, a single light chain binding motif, and a tail region that includes a COOH-terminal SH3 domain. However, myr 3 lacks the regulatory phosphorylation site present in the head domain of protozoan myosin I molecules. Evidence was obtained that the COOH terminus of the tail domain is involved in regulating F-actin binding activity of the NH_2-terminal head domain. The light chain of myr 3 was identified as the Ca^{2+}-binding protein calmodulin. Northern blot and immunoblot analyses revealed that myr 3 is expressed in many tissues and cell lines. Immunofluorescence studies with anti-myr 3 antibodies in NRK cells demonstrated that myr 3 is localized in the cytoplasm and in elongated structures at regions of cell–cell contact. These elongated structures contained F-actin and α-actinin but were devoid of vinculin. Incubation of NRK cells with Con A stimulated the formation of myr 3–containing structures along cell–cell contacts. These results suggest for myr 3 a function mediated by cell–cell contact.

MYOSIN I molecules represent a subfamily of the rapidly expanding myosin superfamily. Like conventional muscle myosin (myosin II), they exhibit an NH_2-terminal head region, a light chain binding region, and a COOH-terminal tail region. The head region is relatively well conserved in all myosins; it comprises ATP- and actin-binding sites and exhibits actin-activated ATPase activity (Pollard et al., 1991). The head region and the light chain–binding region with the associated light chain(s) are sufficient to produce directed force along actin filaments (Toyoshima et al., 1987). The tail regions of myosin I molecules, in contrast to the tail regions of conventional muscle myosin (myosin II), do not dimerize or form filaments. For some of the myosin I tails, it has been demonstrated that they bind to membranes (Adams and Pollard, 1989; Miyata et al., 1989; Hayden et al., 1990). All myosin I tails share a diagnostic myosin I tail homology motif possibly involved in membrane binding (Bähler et al., 1994). A subgroup of myosin I molecules ("amoeboid") identified in *Acanthamoeba castellanii* and *Dictyostelium discoideum* contain in their tail regions a Src homology 3 (SH3) domain. This domain is found in many cytoskeletal and signaling molecules and is thought to represent a regulatory protein–protein interaction motif (Pawson and Schlessinger, 1992).

The amoeboid myosin I subgroup represents the best studied of the myosin I molecules. Their actin-activated ATPase activity and motility are activated by phosphorylation of a single serine/threonine residue in the head region. The light chains associated with the amoeboid myosin I molecules have not been well characterized, and it is currently not known whether they confer additional regulation on motor activity. Other myosins, including myosin I molecules, are known to be regulated via their light chains (Collins et al., 1990).

Localization studies in *Acanthamoeba* provided evidence that myosin I molecules are associated with different intracellular membranes (Gadasi and Korn, 1980; Baines and Korn, 1990; Baines et al., 1992; Yonemura and Pollard, 1992), whereas localization studies in *Dictyostelium* provided evidence that myosin I molecules are concentrated in cortical actin-rich structures, such as leading edge pseudopods and phagocytic cups (Fukui et al., 1989; Jung et al., 1993). Antibody inhibition of myosin IC in *Acanthamoeba* demonstrated a role for this myosin I in contractile vacuole function (Doberstein et al., 1993). Deletions of myosin IA or IB in *Dictyostelium* by homologous recombination resulted in only subtle phenotypes revealing no clear clue as

Address all correspondence to Dr. Martin Bähler, Friedrich-Miescher-Laboratorium, Spemannstrasse 37-39, D-72076 Tübingen, Germany. Tel.: (49) 7071 601 467. Fax: (49) 7071 601 455.

to the specific function of these myosin I molecules (Titus et al., 1993; Jung and Hammer, 1990; Wessels et al., 1991).

If the amoeboid myosin I molecules play general roles in intracellular trafficking of membranes with respect to actin filaments as proposed (Pollard et al., 1991), then these myosins should not be restricted to protozoa. To determine whether such myosin I molecules are involved in aspects of membrane traffic in metazoa, we initiated a search for such molecules in mammalian (rat) tissues. Here we report the identification of an amoeboid-type myosin I from rat. We identified its light chain as calmodulin and demonstrate that this molecule, designated third unconventional myosin from rat (myr 3),[1] is concentrated in cortical actin-rich structures at sites of cell–cell contact. Such structures can be induced at sites of cell–cell contact by application of Con A. A preliminary account of this work has been published in abstract form (Stöffler, H.-E., J. Reinhard, C. Ruppert, and M. Bähler. 1993. *Mol. Biol. Cell.* 4:(Suppl.)39a).

Materials and Methods

Primers and PCR Amplification

PCR was performed with the degenerate oligonucleotides MB11 (sense) 5′-ACGGATCCGGIGCIGGIAA(A/G)ACIGA(A/G)GC-3′, MB 20 (antisense) 5′-CAGAATTCAA(C/T)TCIAT(A/G)TCCAT(G/A)TA(T/C)TTICC-3′, MB 13 (antisense) 5′-ACGGATCCIA(G/A)(T/C)TG(G/A)TA(G/A)AA(T/G/A)AT(G/A)TG(G/A)AA-3′, and MB 14 (sense) 5′-TCGAATTCGA(A/G)GCITT(C/T)GGIAA(C/T)GCIAA-3′ as described by Ruppert et al. (1993). MB 11 was derived from the amino acid sequence GAKTEA, MB 20 from GKYMEIQF, MB13 from FHIFYQL, and MB 14 from EAFGNAK.

Library Screening

A λ ZAP II rat brainstem/spinal cord cDNA library (Stratagene, La Jolla, CA) was screened with a 145-bp PCR fragment (11/20-13) corresponding to nucleotides 609–754 of myr 2 (Ruppert, C., J. Godel, J. Reinhard, and M. Bähler, accession number X74800) according to standard procedures. Several clones were isolated out of 2×10^6 recombinants screened. pBluescript SK plasmids were excised from λ ZAP II clones according to the instructions of the supplier. Clone 33-1, which hybridized with a myr 3 PCR fragment (13/14-1) previously obtained using primers MB 13 and MB 14, was completely sequenced.

DNA Sequencing

Nucleotide sequences were determined by the method of Sanger et al. (1977) using double-stranded DNA templates and the Sequenase version 2.0 kit (United States Biochemicals Corp., Cleveland, OH). For sequencing, a series of nested deletions were constructed by the method of Henikoff (1987) with the Erase-a-Base kit (Promega Corp., Madison, WI). The sequence was determined for both strands. Sequence analysis was performed with the PC/Gene (IntelliGenetics, Mountain View, CA) and the University of Wisconsin Genetics Computer Group (UWGCG version 7) software packages (Devereux et al., 1984).

RNA Purification and Northern Blot Analysis

Total RNA was prepared according to the method of Chirgwin et al. (1979), and poly(A)$^+$RNA was isolated using the PolyATract mRNA isolation system (Promega Corp.). For Northern blot analysis, poly(A)$^+$ RNA was electrophoresed in 1% agarose gels containing 2.2 M formaldehyde and transferred onto Hybond-N nylon membranes (Amersham Buchler GmbH, Braunschweig, FRG). The filters were prehybridized and hybridized at 42°C in 50% formamide, 5× SSC, 50 mM sodium phosphate, pH 7, 0.5% SDS, 0.1 mg/ml poly(A) (Boehringer GmbH, Mannheim, FRG), and 0.25 mg/ml denatured salmon sperm DNA. DNA probes were labeled using a random primer labeling kit (Boehringer GmbH). Filters were washed (2× SSC, 0.1% SDS at room temperature, 2 × 30 min; 2× SSC, 0.1% SDS at 65°C, 10 min) and exposed to X-Omat AR film (Eastman Kodak Co., Rochester, NY) at −70°C with an intensifying screen (Cronex Quanta III, Du Pont, Wilmington, DE).

Antibodies

To raise specific antibodies against myr 3, peptide 1, MEEHPELQQFVGKREKID (corresponding to amino acids 748–765), and peptide 2, RQMDSKWGGKSESIHVT (corresponding to amino acids 326–342), were synthesized. For selective coupling to a carrier protein, a cysteine residue was added to each peptide at the COOH terminus. The peptides were coupled to keyhole limpet hemocyanin (Calbiochem-Behring Co., San Diego, CA) with *m*-maleimidobenzoyl sulfosuccinimide ester (Pierce, Rockford, IL) according to Green et al. (1982) and injected into rabbits using standard immunization protocols. The resulting antisera (peptide 1: Tü 41; peptide 2: Tü 57 and Tü 58) were affinity purified over the respective peptides coupled to CNBr-activated Sepharose 4B (Pharmacia, Freiburg, FRG) according to the instructions of the manufacturer.

Antisera FML 5 and FML 6 were raised against fusion protein S2 (encompassing amino acids 821–1107). Fusion protein S2 was constructed by cloning the BamHI–HindIII fragment of clone 33-1 into the His-tag pQE32 vector (Qiagen, Hilden, FRG). The bacterial fusion protein was affinity purified under denaturing conditions over Ni-NTA resin (Qiagen) as described by the manufacturer and injected into rabbits. Antisera were affinity purified over fusion protein S2 coupled to CNBr-activated Sepharose 4B.

To obtain antibodies directed specifically against the SH3 domain of myr 3, antiserum FML 5 was passed over the GST-SH3 fusion protein coupled to CNBr-activated Sepharose 4B. The cDNA encoding the SH3 domain (amino acids 1057–1105) was amplified by PCR and cloned over BamHI and EcoRI restriction sites into the pGEX-3X vector (Pharmacia).

Immunoblotting

Immunoblotting was performed according to Towbin et al. (1979). Primary antibodies were diluted in 5% nonfat dry milk to 2 μg/ml. Alkaline phosphatase–coupled secondary antibody was diluted in 5% nonfat dry milk and 0.1% Triton X-100. The phosphatase reaction was visualized by the Proto-Blot system (Promega Corp.).

Immunoblotting of calmodulin was performed according to Hulen et al. (1991) with slight modifications. Before electrotransfer, the SDS gel and the methanol-treated Immobilon P membrane (Millipore Corp., Molford, MA) were incubated for 15 min in KP buffer (50 mM potassium phosphate, pH 7.0). After the transfer (4°C, 20 V, 12 h, KP buffer), the membrane was rinsed in PBS, fixed for 45 min with 0.2% glutaraldehyde in KP buffer, and rinsed again in PBS. The membrane was blocked for 1 h in PBS, 2% BSA, 0.1% gelatin. The anti-calmodulin antibody (Sigma, Deisenhofen, FRG) was diluted in PBS; the peroxidase-coupled secondary antibody was diluted in PBS, 0.05% Tween 20. The peroxidase reaction was visualized by the ECL system (Amersham Buchler GmbH).

Immunoprecipitation

Lung tissue of adult rats was homogenized in 0.32 M sucrose, 5 mM Hepes, pH 7.4 (1:5 [wt/vol]), and centrifuged in a SS-34 rotor at 16,000 rpm for 40 min. 1 ml of the supernatant was incubated for 40 min on ice with 10 μg of affinity-purified anti-myr 3 antibody. After addition of 40 μl of protein A–Sepharose 4B (Pharmacia), the mixture was rotated at 4°C for 30 min. The beads were washed three times with TBS (150 mM NaCl 50 mM Tris-HCl, pH 7.4), and bound proteins were eluted by adding 5 μl of 5× SDS buffer and boiling for 5 min.

Calmodulin Binding Assay

Calmodulin gel overlays were performed in the presence and absence of free Ca^{2+} (0.1 mM $CaCl_2$ and 3 mM EGTA, respectively) as described by Slaughter and Means (1987). ^{125}I-labeled calmodulin was purchased from New England Nuclear (Dreieich, FRG).

Immunofluorescence

For indirect immunofluorescence, cells were cultured on coverslips pretreated with poly-L-lysine and fixed in 4% paraformaldehyde in PBS. After quenching with 0.1 M glycine in PBS, the cells were permeabilized for

1. *Abbreviations used in this paper*: myr 3, third unconventional myosin from rat; SH3, Src homology 3.

20 min in 0.1% saponin, 5% normal goat serum in PBS. Primary and secondary antibodies were appropriately diluted in 5% normal goat serum in PBS. Monoclonal antibodies directed against α-actinin and vinculin were purchased from Sigma. Secondary goat anti-rabbit antibodies coupled to rhodamine and goat anti-mouse antibodies coupled to FITC were purchased from Dianova (Hamburg, FRG), FITC-coupled phalloidin was from Molecular Probes, Inc. (Eugene, OR). To remove free antibodies, the cells were rinsed several times with PBS and then mounted (15% Mowiol 4-88 (Hoechst, Frankfurt, FRG), 30% glycerol in PBS, pH 8).

Miscellaneous Techniques

Gel electrophoresis was performed according to Laemmli (1970). Cell lines were grown as described by Bähler et al. (1994). Rat lung tissue was homogenized and extracted as described, and binding to F-actin was assayed by cosedimentation experiments (Ruppert et al., 1993).

Results

Isolation of the Myr 3 cDNA

To identify unconventional myosins expressed in rat brain tissue, PCR amplification of myosin-like sequences was performed. Using degenerate oligonucleotide primers derived from conserved sequences in the myosin head region (GAGKTEA and GKYMDIE), a cDNA fragment coding for a putative myosin was obtained. Screening of a rat brainstem/spinal cord cDNA library with this cDNA fragment led to the identification of several positive clones, encoding four different unconventional myosins (Reinhard, J., A. A. Scheel, C. Ruppert, and M. Bähler. 1993. *Mol. Biol. Cell.* 4:[Suppl.] 40a). One of these clones (33/1; 4.3 kb) strongly hybridized to a cDNA fragment obtained by PCR amplification using primers coding for two different conserved myosin sequences (EAFGNAK and FHIFYQL). This clone, which seemed to encode a novel unconventional myosin, was subjected to DNA sequencing. It exhibited an open reading frame of 3321 bp coding for a protein of 1107 amino acids (Fig. 1). The start of the open reading frame contained the consensus translation initiation sequence described by Kozak (1991). Sequence analysis of the deduced amino acid sequence revealed an NH_2-terminal myosin head domain (amino acids 1–698), a single putative light chain–binding site (amino acids 699–722), and a COOH-terminal tail domain (amino acids 723–1107) (Fig. 2). This myosin was termed myr 3.

Myr 3 Is Related to Myosin I Molecules from Protozoa

Sequence comparison revealed that myr 3 is most similar to human myosin IC (Bement et al., 1994*b*) (95% identity) and chicken BBMIB (Knight, A. E., and J. Kendrick-Jones, accession no. X70400) (73% identity). These three vertebrate myosin I molecules were closely related to myosin I molecules previously characterized in protozoa. Compared with myosin I molecules identified from protozoa, myr 3 was most similar in sequence and structural organization to myosin IB molecules from *A. castellanii* (Jung et al., 1989*b*) and *D. discoideum* (Jung et al., 1989*a*) (Fig. 2).

Similar to myosin IB molecules from *Dictyostelium* and *Acanthamoeba*, the myr 3 motor domain contains a myosin head region (55–57% identity) and only a single IQ motif, which represents a putative light chain–binding site (Figs. 1 and 2). However, in contrast to the myosin I molecules from protozoa, myr 3 is lacking the consensus sequence for phosphorylation in the head region (Fig. 3 *A*). Phosphorylation

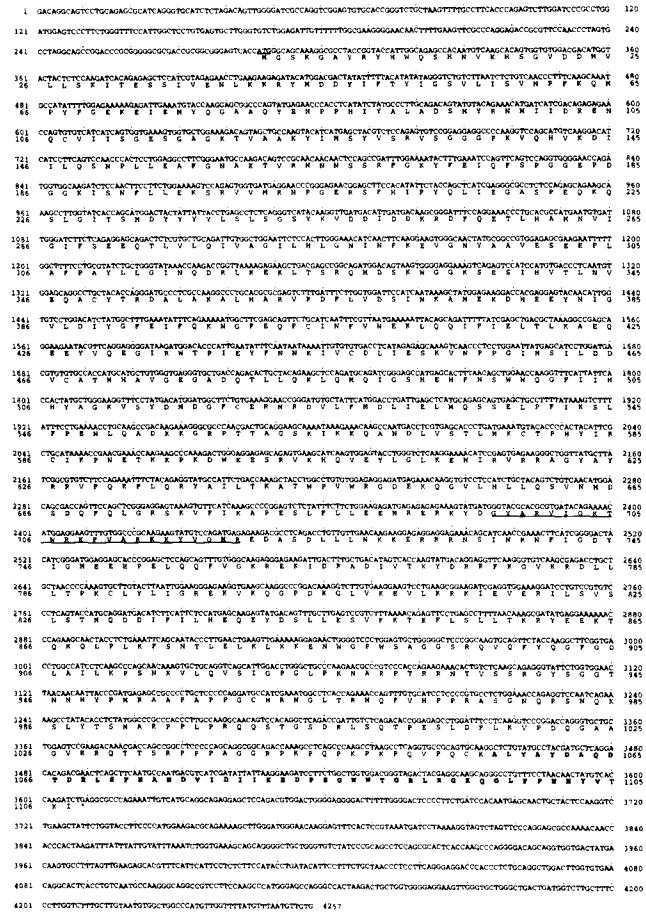

Figure 1. Nucleotide and deduced amino acid sequences of the myr 3 cDNA. The amino acid sequence of myr 3 is shown below the nucleotide sequence. The nucleotides of the start codon at positions 287–289 and the amino acids encompassing the putative light chain–binding region are underlined. Boldfaced amino acids indicate the COOH-terminal SH3 domain. The nucleotide sequence data are accessible through the EMBL nucleotide sequence database under the accession number X74815.

at this site is needed for actin-activated ATPase activity and force production in myosin I molecules from protozoa. Instead, myr 3 exhibits at the corresponding position a negatively charged amino acid, as is also found in myosin II from skeletal muscle, which is constitutively active.

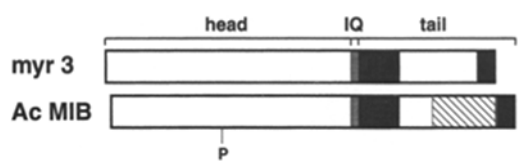

Figure 2. Comparison of the overall structure of myr 3 and myosin IB from *A. castellanii*. Schematic drawings of the heavy chains are shown. IQ motifs are in light gray, the tail homology regions are in dark gray, the SH3 domains are in black, and the GPA-rich region in *Acanthamoeba* myosin IB is crosshatched. The phosphorylation site in Acanthamoeba myosin IB is indicated (*P*). The myosin head domain, the single IQ motif, and the tail region are indicated above the drawing. *Ac MIB, A. castellanii* myosin IB (Jung et al., 1989*b*).

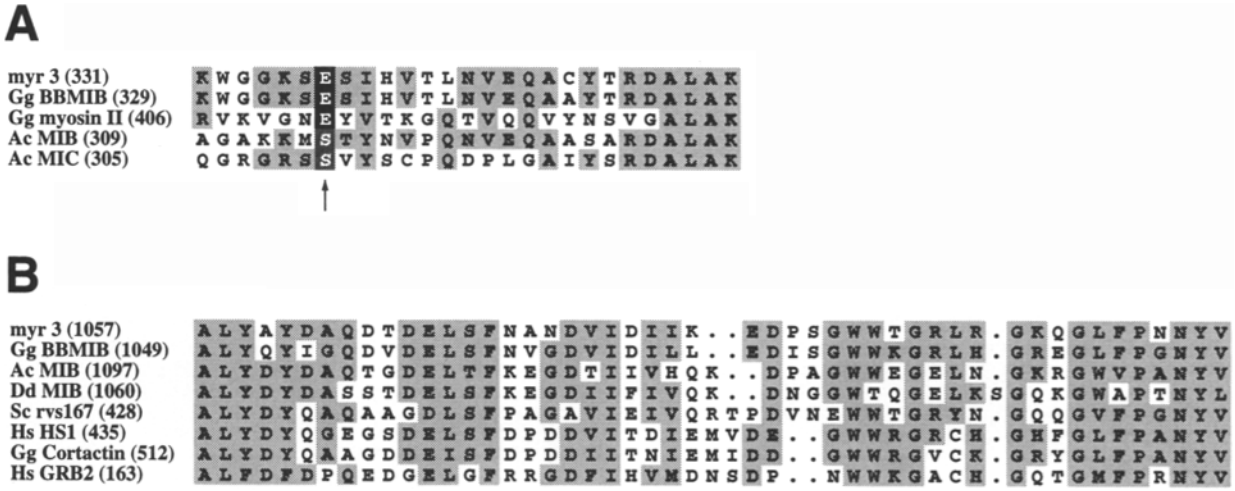

Figure 3. (*A*) Alignment of myosin head amino acid sequences encompassing the phosphorylation site of amoeboid myosin I molecules. Similar residues are on a light gray background. The arrow points to the serine residue that becomes phosphorylated in myosins IB and IC of *A. castellanii*. The serine residues are rendered in white against a dark gray background, and the glutamic acid residues at the corresponding positions in the vertebrate myosins in white against a black background. The numbers refer to the position of the first displayed amino acid. *Gg BBMIB*, chicken brush border myosin IB (Knight, A. E., and J. Kendrick-Jones, accession number X70400); *Gg myosin II*, conventional myosin II from chicken fast skeletal muscle (Molina et al., 1987); *Ac MIB*, *A. castellanii* myosin IB (Jung et al., 1989*b*); *Ac MIC*, *A. castellanii* myosin IC (Jung et al., 1987). (*B*) Alignment of the myr 3 SH3 domain amino acid sequence with closely related SH3 domains. Similar residues are shaded with a gray background. The numbers refer to the position of the first displayed amino acid. *Gg BBMIB*, chicken brush border myosin IB (Knight and Kendrick-Jones, accession number X70400); *Ac MIB*, *A. castellanii* myosin IB (Jung et al., 1989*b*); *Dd MIB*, *D. discoideum* myosin IB (Jung et al., 1989*a*); *Sc rvs167*, yeast rvs167 (Bauer et al., 1993); *Hs HSI*, human hematopoietic lineage cell-specific protein 1 (Kitamura et al., 1989); *Gg Cortactin*, chicken cortactin (p80/85) (Wu et al., 1991); *Hs GRB2*, human growth factor receptor-bound protein 2 (Lowenstein et al., 1992; Matuoka et al., 1992).

The tail domain of myr 3 shares 33–34% sequence identity with the tail domains of *Acanthamoeba* and *Dictyostelium* myosin IB. As in these protozoan myosin molecules, the myosin I tail homology motif, as defined by Bähler et al. (1994), is found at the NH_2 terminus of the tail domain, and the second and third blocks of conserved residues are separated by a highly charged insertion. The relative position and subdivision of this motif represent further diagnostic criteria for subclassification of myosin I proteins. Unlike the tail domains of the protozoan myosin I molecules, the myr 3 tail does not contain an extended region rich in GPA/Q. However, it exhibits a short stretch of PK/Q dipeptide repeats. At its COOH terminus, following this dipeptide repeat, myr 3 has an SH3 domain (Fig. 3 *B*). This domain is found in many proteins that are involved in cell signaling and/or interact with the actin cytoskeleton (Pawson and Schlessinger, 1992). It is thought to represent a protein–protein interaction motif. The myr 3 SH3 domain is most similar to the SH3 domains found in myosin I molecules from protozoa, other cytoskeletal proteins, and the COOH-terminal SH3 domain of GRB2 (Fig. 3 *B*).

Myr 3 Is Expressed in Many Tissues and Cell Lines

Northern blot analysis of poly(A)$^+$ RNA from neonatal and adult rat tissues revealed a message size of 5.1 kb. Myr 3 message was detected in several tissues (Fig. 4), such as neonatal kidney, lung, and intestine, as well as in adult lung and spleen.

Antisera raised against synthetic peptides and a fusion protein encompassing various regions of myr 3 (see Materials and Methods) specifically recognized a protein of 126 kD in several rat tissues and cell lines of rat, mouse, dog, and human origin (Figs. 5 and 6 and data not shown). This molecular mass is in good agreement with the calculated mass from the deduced amino acid sequence of 126.8 kD. In some tissues and cell lines, anti-myr 3 antibodies also recognized a band of 110 kD. This band became more evident with time of storage, and at the same time, the band at 126 kD decreased in intensity (Fig. 7 *A*). This result strongly suggested that the 110-kD band represents a degradation product. Indeed, antibodies directed against the COOH-terminal SH3 domain did not recognize the 110-kD band, demonstrating that myr 3 was degraded from the COOH terminus (Fig. 7 *A*). The relative amount of myr 3 degradation strongly depended on the source of tissue. Rapid degradation was observed in spleen (Fig. 7 *A*), whereas myr 3 degradation was less pronounced in lung tissue (Fig. 7, *B* and *C*). In conclusion, myr 3 exhibited a widespread distribution.

Loss of a COOH-terminal Fragment Influences Solubilization and F-Actin Binding of Myr 3

Upon homogenization of rat lung tissue, the bulk of myr 3 was recovered in the soluble fraction and a smaller amount was found in the particulate fraction (Fig. 7 *B*). The reverse distribution was observed for a 110-kD NH_2-terminal fragment that is missing part of the COOH-terminal tail region, including the SH3 domain (Fig. 7, *A* and *B*). This 110-kD NH_2-terminal fragment was more abundant in the particulate fraction, from which it was released by Mg-ATP. This result suggested that in tissue homogenates the 110-kD

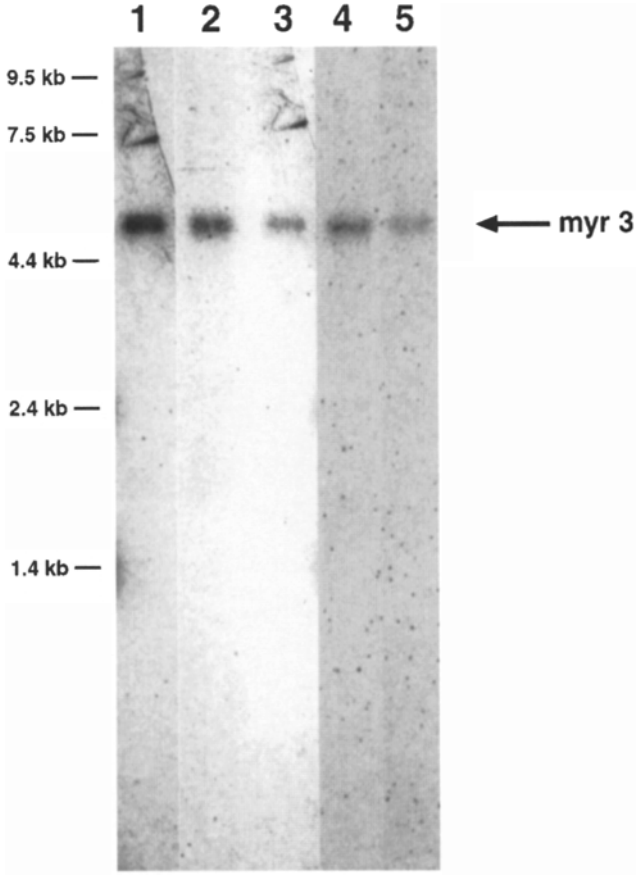

Figure 4. Message size and expression pattern of myr 3 mRNA. Northern blots (1 μg of poly(A)$^+$ RNA per lane) were hybridized with the PCR fragment 13/14-1. The position of the 5.1-kb myr 3 mRNA is indicated on the right; size standards are on the left. The tissues used were kidney (lane *1*), lung (lane *2*), and intestine (lane *3*) from neonatal rats and spleen (lane *4*) and lung (lane *5*) from adult rats.

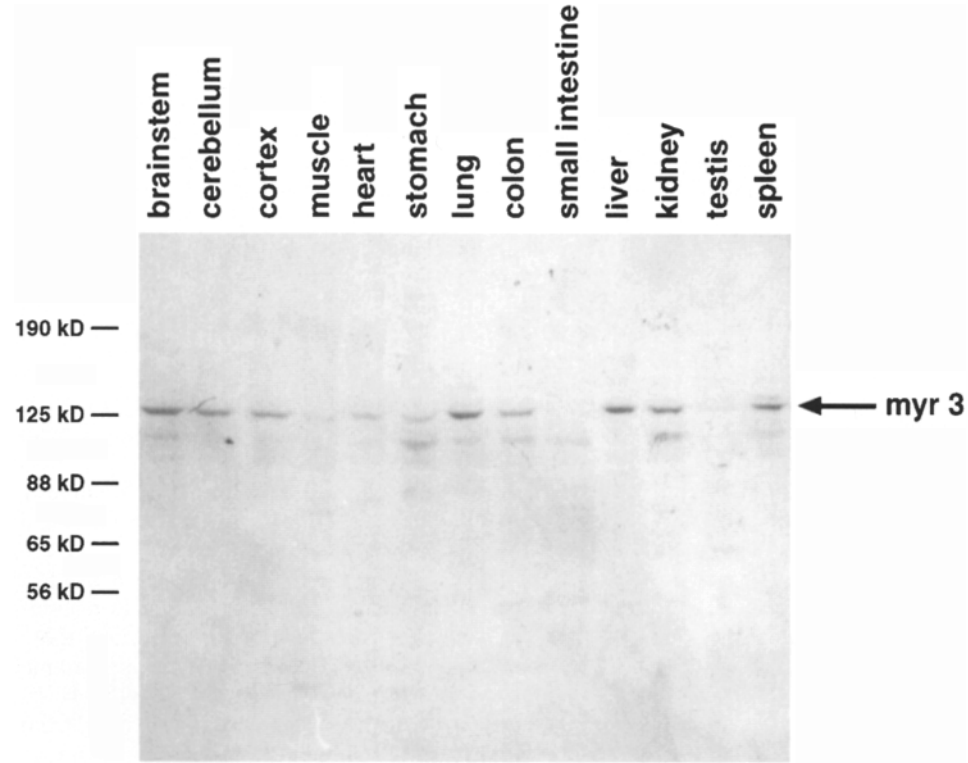

Figure 5. Tissue distribution of myr 3. Equal amounts of protein from the indicated tissues were separated on SDS-PAGE and immunoblotted with the affinity-purified antibody Tü 58 followed by a secondary antibody coupled to alkaline phosphatase. The position of myr 3 is indicated on the right; molecular mass standards are on the left. Tissues are indicated above each lane.

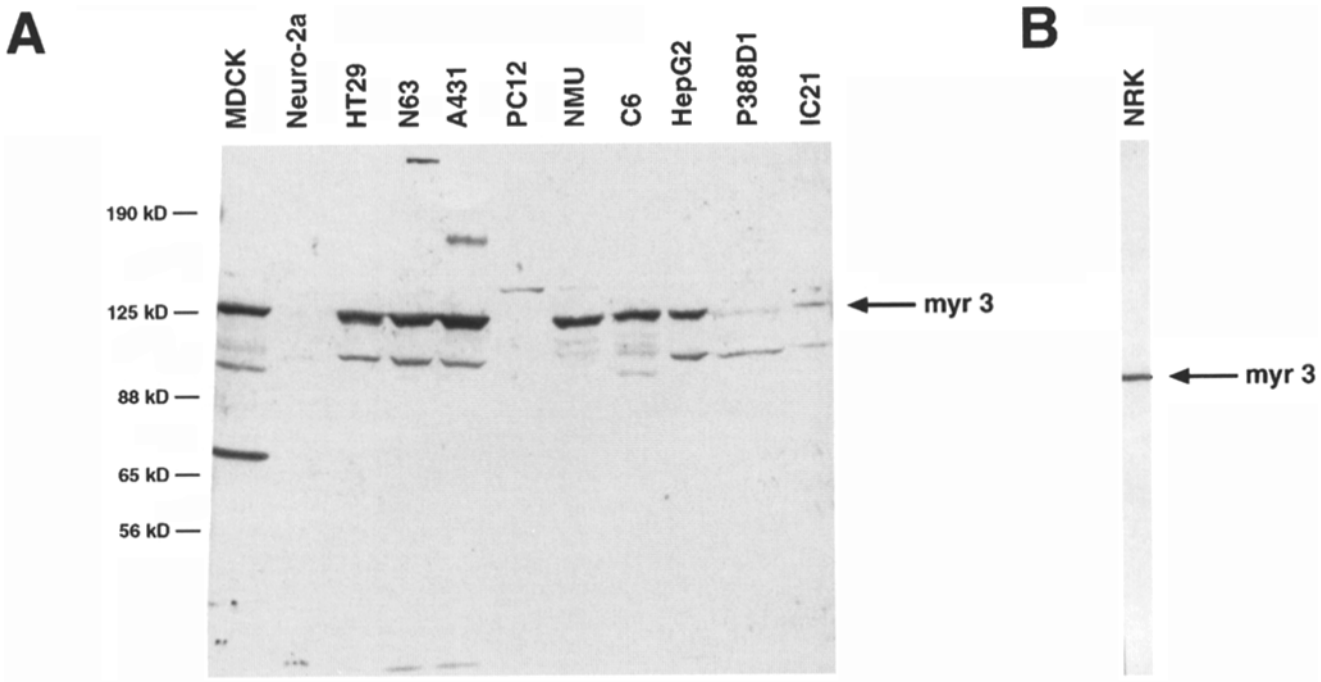

Figure 6. Expression of myr 3 in different cell lines. (*A*) Equal amounts of protein from the indicated cell lines were separated on SDS-PAGE and immunoblotted with the affinity-purified antibody Tü 41. (*B*) Homogenate from NRK cells was separated on SDS-PAGE and immunoblotted with the affinity-purified antibody FML 6. The primary antibody was followed by a secondary antibody coupled to alkaline phosphatase. The position of myr 3 is indicated on the right; molecular weight standards are on the left. Cell lines are indicated on top of each lane. *MDCK*, Madin–Darby canine kidney cells; *Neuro-2a*, mouse, neuroblastoma; *HT29*, human, colon adenocarcinoma; *N63*, human, glioblastoma; *A431*, human, epidermal carcinoma; *PC12*, rat, adrenal phaeochromocytoma; *NMU*, rat, breast adenocarcinoma; *C6*, rat, glial tumor; *HepG2*, human, liver tumor; *P388D1*, mouse, monocyte–macrophage; *IC21*, mouse, macrophage; *NRK*, rat, kidney fibroblast.

NH_2-terminal fragment, but not intact myr 3, was binding in an ATP-regulated manner to F-actin.

To test this suggestion directly, the soluble fraction was incubated in the presence or absence of polymerized actin and ATP, respectively. As demonstrated in Fig. 7 *C*, the 110-kD NH_2-terminal fragment cosedimented in an ATP-regulated manner with F-actin, whereas intact myr 3 showed virtually no ability to cosediment with F-actin. This result demonstrated that in tissue homogenates the COOH terminus of myr 3 was inhibiting the ATP-regulated F-actin binding activity of myr 3.

Myr 3 Is Associated with Calmodulin

To identify the putative light chain associated with myr 3, we performed immunoprecipitation experiments. Antisera Tü 57 and FML 6 were shown to precipitate myr 3 under nondenaturing conditions. Antiserum Tü 41 reacted with myr 3 on immunoblots but was unable to precipitate myr 3 under nondenaturing conditions (Fig. 8 *A*). Immunoprecipitation experiments with antisera Tü 57 and FML 6 (but not Tü 41) from [^{35}S]methionine-labeled NRK and C6 cells led to the coprecipitation of a band comigrating with authentic calmodulin (data not shown). To probe directly for coprecipitation of calmodulin with myr 3, immunoprecipitates from lung tissue were analyzed by immunoblotting with anti-calmodulin antibodies. In immunoprecipitates of myr 3 with antibodies Tü 57 and FML 6, a band exhibiting the Ca^{2+}-dependent mobility shift on SDS-PAGE characteristic of calmodulin was recognized by the anti-calmodulin antibody (Fig. 8 *B*). This result strongly suggested that myr 3 was associated with calmodulin.

To test directly whether myr 3 is a calmodulin-binding protein, gel overlay assays with ^{125}I-labeled calmodulin were performed. Aliquots of analogous immunoprecipitates probed with the anti-calmodulin antibody were separated on SDS-PAGE and incubated with ^{125}I-labeled calmodulin in the presence (0.1 mM $CaCl_2$) or absence (3 mM EGTA) of free Ca^{2+} (Fig. 8 *C*). ^{125}I-labeled calmodulin interacted with myr 3 in both the presence and absence of free Ca^{2+}, as is characteristic of myosin light chains.

Intracellular Localization of Myr 3

To determine the intracellular localization of myr 3, indirect immunofluorescence experiments were performed with NRK cells. Indirect immunofluorescence staining obtained with the FML 6 antibody, which is highly specific for myr 3 in NRK cells, (Fig. 6 *B*) is shown. This anti-myr 3 antibody prominently stained short, elongated structures located close to sites of cell–cell contacts (Fig. 9, *A*, *C*, and *E*). These myr 3–positive structures were found only at a subset of cell–cell contacts, indicating that they might form transiently during cell–cell contact formation. Besides these prominently labeled structures, a general punctate staining of the cytoplasm was also observed (Fig. 9). Antibody Tü 58, which was raised against a synthetic peptide derived from an actin-binding region in the head domain, gave a similar

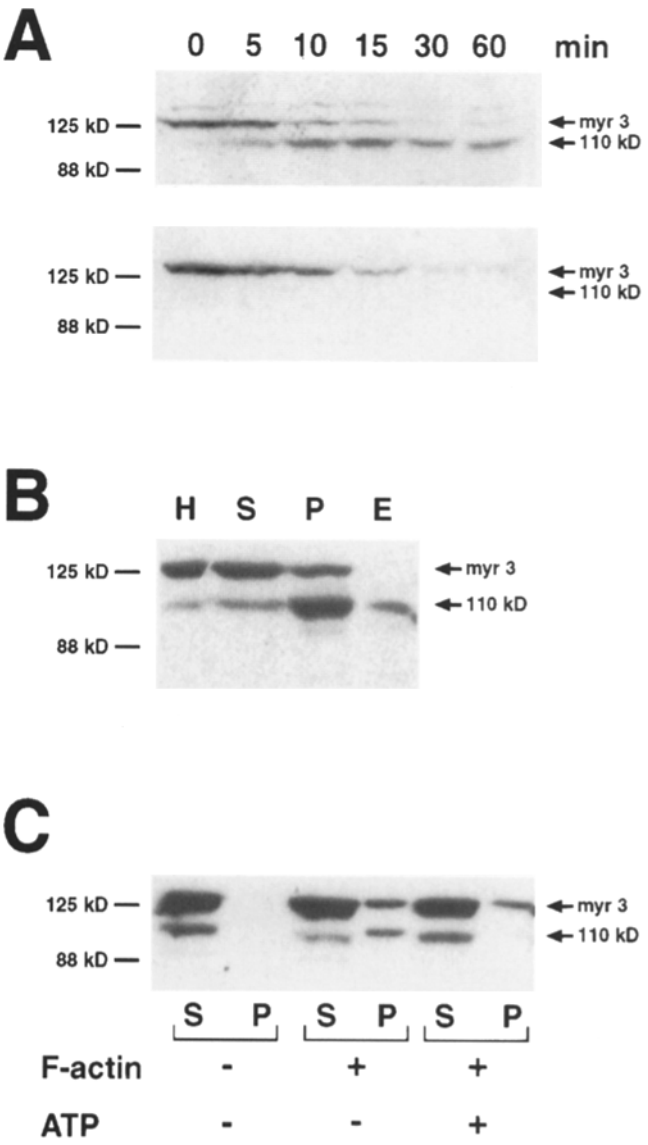

Figure 7. Characterization of myr 3 and a 110-kD NH_2-terminal fragment. (*A*) Myr 3 is rapidly degraded in spleen tissue to a 110-kD fragment lacking the COOH-terminal SH3 domain. Spleen from adult rats was homogenized in 0.32 M sucrose, 5 mM Hepes, pH 7.4, and incubated at room temperature. At various time points, indicated above each lane, samples were collected and analyzed by immunoblotting with antibodies Tü 41 (*top panel*) and FML5 affinity-purified over a GST-SH3 fusion protein (*bottom panel*). The arrows on the right indicate the positions of myr 3 and its 110-kD degradation product; molecular mass standards are shown on the left. (*B*) Different solubilization properties of myr 3 and the 110-kD NH_2-terminal fragment. Lung tissue from adult rats was homogenized in a buffer containing 20 mM Hepes, pH 7.4, 10 mM $MgCl_2$, 1 mM 2-mercaptoethanol, 0.1 mM EGTA, and 100 mM NaCl (*H*) and centrifuged to obtain supernatant (*S*) and pellet (*P*). The pellet was extracted with the same buffer containing 5 mM ATP (*E*). The obtained fractions were analyzed for myr 3 distribution by immunoblotting with antibody Tü 41. (*C*) The 110-kD NH_2-terminal fragment but not intact myr 3 binds in an ATP-regulated manner to F-actin. Lung tissue from adult rats was homogenized in 0.32 M sucrose, 5 mM Hepes, pH 7.4, and centrifuged. The supernatant was incubated in the absence (−) or presence (+) of actin (5 μM) and ATP (2 mM). F-actin binding was assayed by cosedimentation with F-actin. Supernatants (*S*) and pellets (*P*) were analyzed by immunoblotting with antibody Tü 41.

staining pattern. However, the elongated structures at cell–cell contacts were less prominently stained (data not shown).

To characterize these myr 3–positive structures at cell–cell contacts, double immunofluorescence experiments were performed. Because myr 3 is postulated to produce force along actin filaments, cells were simultaneously labeled for myr 3 and F-actin (Fig. 9, *A* and *B*). The structures labeled with anti–myr 3 antibody were also positive for F-actin. However, these structures represented only a fraction of the total F-actin present in a cell. The individual structures containing myr 3 and F-actin exhibited the appearance of cross-linked actin filaments. Therefore, double immunofluorescence staining for myr 3 and the F-actin cross-linking protein α-actinin were performed (Fig. 9, *C* and *D*). These experiments demonstrated that the structures labeled by anti–myr 3 antibodies at cell–cell contacts were also labeled by antibodies against α-actinin. These results suggested that myr 3 colocalizes with actin filament–α-actinin networks at sites of cell–cell contact. Because the myr 3–positive structures were reminiscent of focal adhesions, we performed double immunofluorescence experiments with an antibody directed against vinculin, an essential component of focal adhesions. As shown in Fig. 9, *E* and *F*, the myr 3–positive structures did not colocalize with focal adhesions when stained by anti-vinculin antibodies and therefore did not represent focal adhesions.

Since myr 3 is enriched in presumably transient structures at sites of cell–cell contact, we reasoned that this localization might be regulated by cell surface receptors. To test this possibility, NRK cells were incubated with the plant lectin Con A. Con A binds tightly to mannose and glucose moieties of cell surface receptors and activates them upon binding. A dramatic induction of myr 3 localization along cell–cell contacts was observed as a consequence of Con A treatment of NRK cells (Fig. 10). Whereas in untreated cells myr 3–containing structures at sites of cell–cell contact were only occasionally observed, in Con A–treated cells myr 3 staining outlined cell–cell borders in a zipper-like appearance. The organization of F-actin was also modulated in Con A–treated cells, and similar structures colocalizing with myr 3 were observed along cell–cell borders (Fig. 10, *A* and *B*). There were no myr 3–positive structures induced with Con A at sites other than cell–cell borders. In control experiments we found that application of Con A did not result in the relocalization of two other myosin I molecules, namely myr 1 and myr 2, to these structures. In summary, myr 3 was concentrated in Con A–inducible F-actin–rich structures at regions of cell–cell contact.

Discussion

Our identification of a mammalian myosin I related to myosin I molecules from protozoa demonstrates a ubiquitous distribution for this subfamily of myosin I proteins and implies that they are of general importance for cellular function. This is a notion strengthened by the recent deposition of the sequence for chicken brush border myosin IB in the database by A. E. Knight and J. Kendrick-Jones (accession number X70400) and the cloning of human myosin IC (Bement et al., 1994*b*). Whereas human myosin IC represents the human homolog of rat myr 3, chicken brush border myosin IB is more likely a direct homolog of a different human

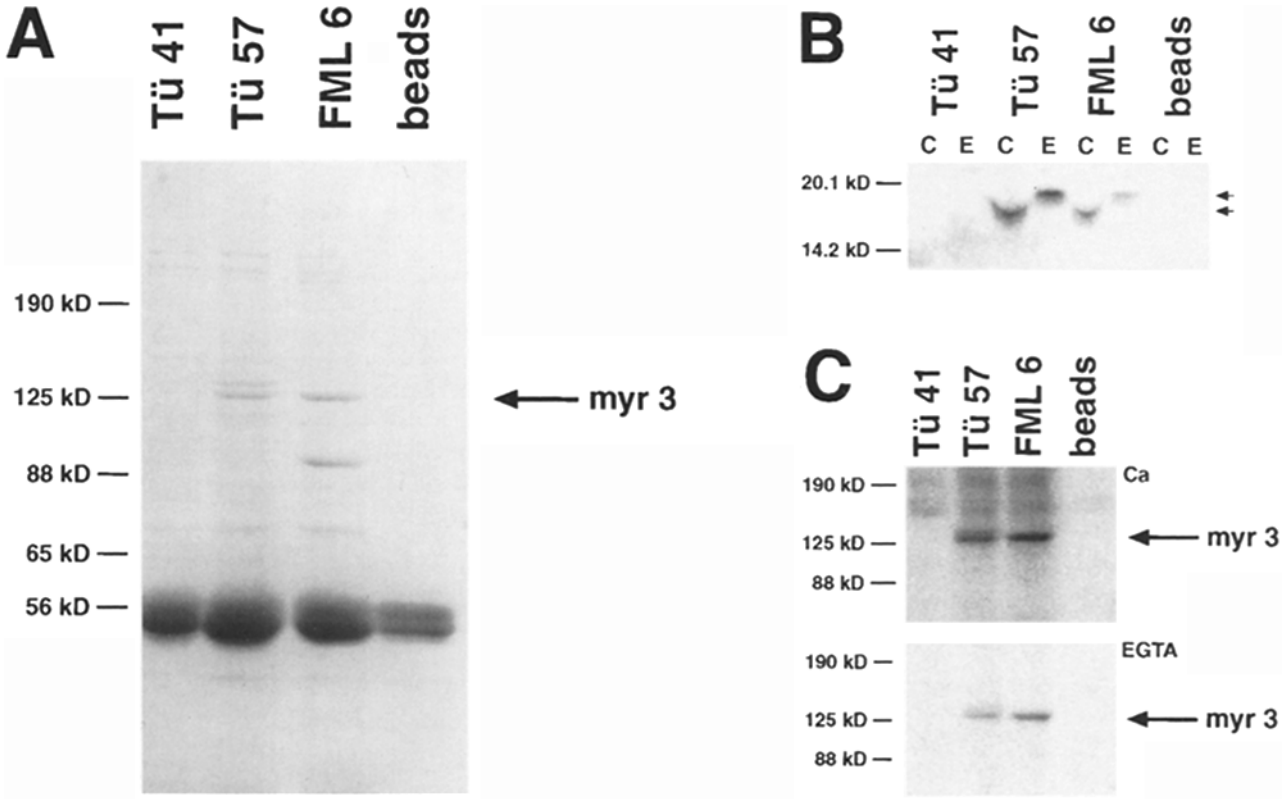

Figure 8. Coprecipitation of calmodulin with myr 3 and direct binding of calmodulin to myr 3. Myr 3 was immunoprecipitated from adult rat lung tissue homogenates with affinity-purified anti–myr 3 antibodies Tü 41, Tü 57, and FML 6; immunoprecipitation only with protein A–Sepharose beads served as a control. (*A*) Immunoprecipitates were separated on SDS- PAGE, and proteins were stained with Coomassie brilliant blue. The arrow on the right indicates the position of myr 3; molecular mass standards are shown on the left. The antibodies used are indicated above each lane. (*B*) Immunoprecipitates were boiled with 5× Laemmli buffer in the presence (*C*) or absence (*E*) of free Ca^{2+}, separated on SDS-PAGE, and immunoblotted with an anti-calmodulin antibody followed by a secondary antibody coupled to peroxidase. The two arrowheads on the right indicate the relative positions of authentic calmodulin in the presence (*bottom arrowhead*) and absence (*top arrowhead*) of free Ca^{2+}. Protein standards are indicated on the left, and the antibodies used for immunoprecipitation are above each lane. (*C*) Immunoprecipitates identical to those in *A* were separated on SDS-PAGE and incubated with ^{125}I-calmodulin in the presence (*top panel*; *Ca*) or absence (*bottom panel*; *EGTA*) of free Ca^{2+}. The autoradiographs are shown. Protein standards are indicated on the left; the antibodies used for immunoprecipitation are above each lane.

myosin I, myosin ID (Bement et al., 1994*a*), and therefore is not the direct chicken homolog of rat myr 3. Thus, amoeboid myosin I molecules are not restricted to protozoa.

The motor activity of protozoan myosin I molecules is activated by phosphorylation of a single serine/threonine residue in the head region (Maruta and Korn, 1977; Brzeska et al., 1989). This region of the head is proposed to be part of the primary actin-binding site (Rayment et al., 1993; Schröder et al., 1993). A consensus sequence that serves as a substrate recognition motif for the myosin I heavy chain kinase has been determined (Brzeska et al., 1990). The corresponding region in myr 3 does not conform to this consensus phosphorylation sequence. It contains at the position of a serine or threonine residue a negatively charged glutamic acid residue, as is also found in conventional myosin. This negatively charged residue might substitute for the negative charge introduced by a phosphate group. It is therefore likely that myr 3 motor activity, as in conventional myosin, is regulated by other means. Two possibilities may represent regulation through the light chain in the neck region and/or the SH3 domain at the COOH terminus.

In this report we demonstrated that upon immunopurification of myr 3, the Ca^{2+}-binding protein calmodulin is copurified and that purified myr 3 can bind calmodulin in gel overlay assays. These data strongly suggest that one calmodulin molecule is associated with the single light chain–binding site (IQ motif) present in myr 3. The association of calmodulin with myr 3 and the binding of calmodulin to myr 3 were not dependent on free Ca^{2+} concentrations, which is consistent with the notion that calmodulin acts as a light chain and binds to the IQ motif. IQ motifs were reported to bind calmodulin even in the absence of free Ca^{2+} (Halsall and Hammer, 1990). Calmodulin has been demonstrated to serve as the light chain for several unconventional myosin molecules, including other vertebrate myosin I molecules. However, calmodulin has not yet been reported to act as the light chain for amoeboid myosin I molecules. Purified myosin IB from *Acanthamoeba* was reported to contain a single light chain of 27 kD (Maruta et al., 1978), and myosin IC contains two light chains of 14 kD (Lynch et al., 1989). These molecular masses are at variance with the molecular mass of calmodulin, which is 17 kD. The pro-

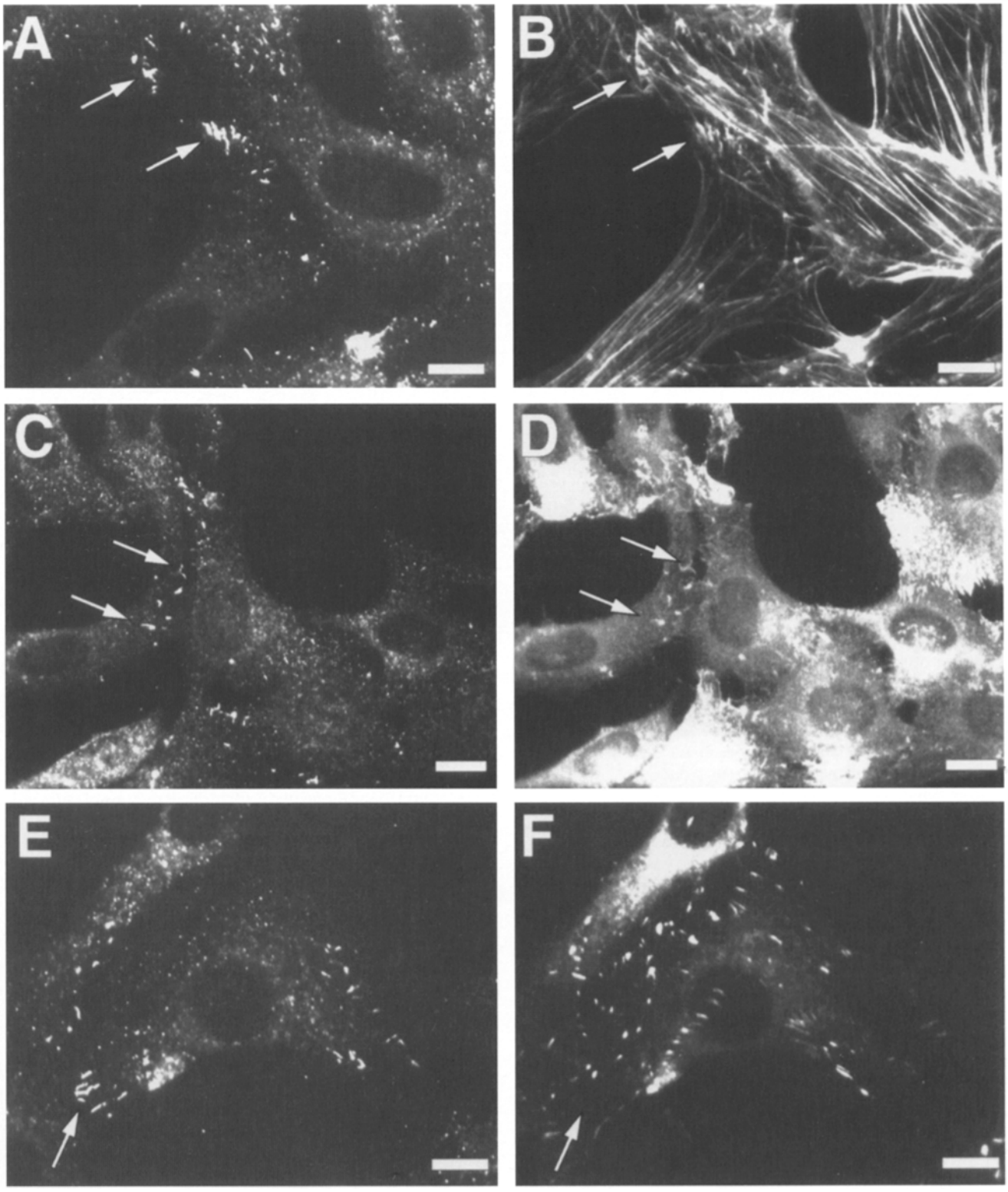

Figure 9. Double immunofluorescence localization of myr 3 with F-actin, α-actinin, and vinculin in NRK cells. Cells were fixed with 4% paraformaldehyde, permeabilized with 0.1% saponin, and stained with the rabbit anti-myr 3 antibody FML 6 (*A*, *C*, and *E*) followed by rhodamine-coupled goat anti-rabbit antibody. Double staining was performed with FITC-coupled phalloidin (*B*), mouse anti-α-actinin antibody (*D*), and mouse anti-vinculin antibody (*F*) followed by FITC-coupled goat anti-mouse antibody. The arrows point to regions of elongated structures enriched in myr 3. These structures were also detected to contain F-actin (*A* and *B*) and α-actinin (*C* and *D*), but not vinculin (*E* and *F*). Bars, 10 μm.

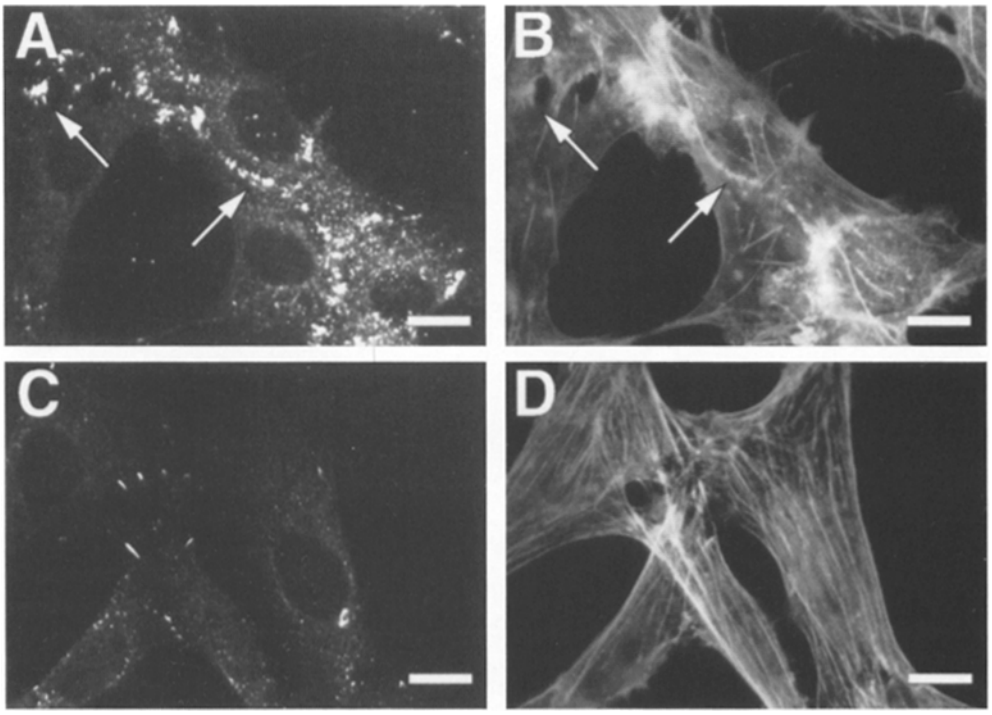

Figure 10. Con A-induced myr 3 localization at cell-cell boundaries in NRK cells. NRK cells were incubated for 30 min with PBS in the presence (*A* and *B*) or absence (*C* and *D*) of Con A (5 μg/ml) and then fixed with 4% paraformaldehyde, permeabilized with 0.1% saponin, and stained with the rabbit anti-myr 3 antibody FML 6 followed by rhodamine-coupled goat anti-rabbit antibody (*A* and *C*) and with FITC-coupled phalloidin (*B* and *D*). The arrows in *A* and *B* point to cell boundaries that are outlined by myr 3- and F-actin-positive structures after treatment with Con A. Bars, 10 μm.

posed difference in the mechanism(s) regulating motor activity of protozoan myosin I molecules and of myr 3 might have caused the need for different light chains. Instead of being regulated by phosphorylation of the head region, myr 3 could be regulated by Ca^{2+} binding to calmodulin. This possibility is not unprecedented. Ca^{2+} has been demonstrated to regulate motility of brush border myosin I and myosin V, both of which have calmodulin as light chains associated with them (Collins et al., 1990; Cheney et al., 1993).

The SH3 domain found at the COOH terminus of myr 3 represents another domain possibly involved in the regulation of myr 3 function. SH3 domains have been reported to act and interact intramolecularly and to be masked until activation exposes them for interaction with a target protein (Murphy et al., 1993; Okada et al., 1993; Superti-Furga et al., 1993). Indeed, the myr 3 tail region exhibits proline-rich sequences that could possibly interact with the SH3 domain. Proline-rich sequences have recently been demonstrated to serve as ligands for several SH3 domains (Cicchetti et al., 1992; Ren et al., 1993). In favor of such a hypothesis is our finding that most myr 3 is cytosolic after cell homogenization and does not seem to be able to interact with actin filaments. However, a breakdown product of myr 3 (110-kD NH_2-terminal fragment) that has lost its SH3 domain is interacting with actin filaments in an ATP-regulated manner. Therefore, the SH3 domain might also be a candidate region for regulating myr 3 activity.

The SH3 domain of myr 3 might alternatively or in addition serve as a regulatory targeting module for myr 3 localization. It was recently reported that the SH3 domain of fodrin localizes to the leading lamellae of locomoting fibroblasts (Meriläinen et al., 1993) and that the two SH3 domains of GRB2 are necessary for the localization of microinjected GST-GRB2 fusion protein to membrane ruffles (Bar-Sagi et al., 1993).

Immunofluorescence localization of myr 3 in NRK cells revealed a punctate cytosolic staining in all cells and a prominent staining of distinct elongated structures at occasional sites of cell-cell contacts. The punctate staining seemed to be homogeneously distributed throughout the cytoplasm. This cytoplasmic staining may represent a pool of inactive myr 3 that in response to a certain stimulus (see below) may be recruited to the elongated structures in regions of cell-cell contact. Support for this hypothesis is provided by our observation that the punctate staining of myr 3 is reduced around the elongated structures containing myr 3.

The elongated structures at sites of cell-cell contact stained by anti-myr 3 antibodies were enriched for F-actin and α-actinin. Therefore, these structures consist of cross-linked actin filament networks. However, these myr 3-positive structures do not represent focal adhesions because no colocalization with vinculin, a marker for focal adhesions, could be observed. It remains to be determined whether myr 3 is part of the actin network and may cross-link and move actin filaments relative to each other by interacting through its tail domain with actin or an actin-associated protein or whether myr 3 is associated with a membrane protein that might get drawn to this actin-rich structures by myr 3. The myr 3 tail domain contains a region that is homologous to a region in amoeboid myosin I molecules implicated in membrane binding (Doberstein and Pollard, 1992) but contains no extended glycine/proline-rich region implicated in nucleotide-insensitive actin binding (Jung and Hammer, 1994; Rosenfeld and Rener, 1994).

Myr 3 is related to myosin IB proteins from *A. castellanii* and *D. discoideum*. The localizations reported for these protozoan myosin I molecules differed from the localization of myr 3. Myosin IB from *Acanthamoeba* has been localized to the plasma membrane, large vacuole membranes, phagocytic membranes, and cytoplasm (Baines et al., 1992). Myo-

sin IB from *Dictyostelium* was localized to the leading edge and phagocytic cups (Fukui et al., 1989; Jung et al., 1993). No particular staining of the leading edge or the plasma membrane using antibodies against myr 3 was detected in NRK cells. These differences in localization between myr 3 and homologous protozoan myosin I molecules might represent functional adaptations to a multicellular organism. Interestingly, expression of *Dictyostelium* myosin IB is increased severalfold upon starvation-induced chemotactic aggregation (Jung et al., 1989a). Localization of a myosin I at cell–cell contacts, however, is not unprecedented since myosin IA from *A. castellanii*, from which no complete sequence has been determined, has been found at phase-dense cortical structures at sites of cell–cell contact (Yonemura and Pollard, 1992).

Treatment of NRK cells with Con A resulted in a dramatic induction of myr 3– and F-actin–positive structures along cell–cell contacts exhibiting a zipper-like appearance. The induced structures resembled the myr 3–containing structures in untreated cells but were on average somewhat shorter. The restriction of these structures to areas of cell–cell contact independently of Con A treatment implies that Con A enhances a physiologic signal. It is not clear whether recruitment of myr 3 represents the cause for these structures or the consequence of the formation of these F-actin–containing structures. However, it seems likely that myr 3 function is regulated by cell surface–mediated signaling events possibly involving the SH3 domain in the myr 3 tail. It remains to be determined whether myr 3 plays a role in promoting or inhibiting cell–cell contact formation.

We thank Christa Baradoy, Jasminca Godel, and Iris Kehrer for skillful technical assistance. Bill M. Bement and Mark Mooseker kindly shared unpublished sequence information.

Received for publication 22 November 1994 and in revised form 26 January 1995.

References

Adams, R. J., and T. D. Pollard. 1989. Binding of myosin-I to membrane lipids. *Nature (Lond.).* 340:565–588.

Bähler, M., R. Kroschewski, H.-E. Stöffler, and T. Behrmann. 1994. Rat myr 4 defines a novel subclass of myosin-I: identification, distribution, localization and mapping of calmodulin binding sites with differential calcium sensitivity. *J. Cell Biol.* 126:375–389.

Baines, I. C., and E. D. Korn. 1990. Localization of myosin IC and myosin II in *Acanthamoeba castellanii* by indirect immunofluorescence and immunogold electron microscopy. *J. Cell Biol.* 111:1896–1904.

Baines, I. C., H. Brzeska, and E. D. Korn. 1992. Differential localization of Acanthamoeba myosin I isoforms. *J. Cell Biol.* 119:1193–1203.

Bar-Sagi, D., D. Rotin, A. Batzer, V. Mandiyan, and J. Schlessinger. 1993. SH3 domains direct cellular localization of signaling molecules. *Cell.* 74:83–91.

Bauer, F., M. Urdaci, M. Aigle, and M. Crouzet. 1993. Alteration of a yeast SH3 protein leads to conditional viability with defects in cytoskeletal and budding patterns. *Mol. Cell. Biol.* 13:5070–5084.

Bement, W. M., T. Hasson, J. A. Wirth, R. E. Cheney, and M. S. Mooseker. 1994*a*. Identification and overlapping expression of multiple unconventional myosin genes in vertebrate cell types. *Proc. Natl. Acad. Sci. USA.* 91: 6549–6553.

Bement, W. M., J. A. Wirth, and M. S. Mooseker. 1994*b*. Cloning and mRNA expression of human unconventional myosin-IC. *J. Mol. Biol.* 243:356–363.

Brzeska, H., T. J. Lynch, B. Martin, and E. D. Korn. 1989. The localization and sequence of the phosphorylation sites of Acanthamoeba myosins I. An improved method for locating the phosphorylated amino acid. *J. Biol. Chem.* 264:19340–19348.

Brzeska, H., T. J. Lynch, B. Martin, A. Corigliano-Murphy, and E. D. Korn. 1990. Substrate sepecificity of Acanthamoeba myosin I heavy chain kinase as determined with synthetic peptides. *J. Biol. Chem.* 265:16138–16144.

Cheney, R. E., M. K. O'Shea, J. E. Heuser, M. V. Coelho, J. S. Wolenski, E. M. Espreafico, P. Forscher, R. E. Larson, and M. S. Mooseker. 1993. Brain myosin-V is a two-headed unconventional myosin with motor activity. *Cell.* 75:13–23.

Chirgwin, J. M., A. E. Przybala, R. Y. MacDonald, and W. J. Rüttner. 1979. Isolation of biologically active ribonucleic acid from sources enriched in ribonuclease. *Biochemistry.* 18:5294–5299.

Cicchetti, P., B. J. Mayer, G. Thiel, and D. Baltimore. 1992. Identification of a protein that binds to the SH3 region of Abl and is similar to Bcr and GAP-rho. *Science (Wash. DC).* 257:803–806.

Collins, K., J. R. Sellers, and P. T. Matsudaira. 1990. Calmodulin dissociation regulates brush border myosin I (110-kD- calmodulin) mechanochemical activity in vitro. *J. Cell Biol.* 110:1137–1147.

Devereux, J., P. Haeberli, and O. Smithies. 1984. A comprehensive set of sequence analysis programs for the VAX. *Nucleic Acids Res.* 12:387–395.

Doberstein, S., and T. D. Pollard. 1992. Localization and specificity of the phospholipid and actin binding sites on the tail of Acanthamoeba myosin IC. *J. Cell Biol.* 117:1241–1249.

Doberstein, S. K., I. C. Baines, G. Wiegand, E. D. Korn, and T. D. Pollard. 1993. Inhibition of contractile vacuole function in vivo by antibodies against myosin-I. *Nature (Lond.).* 365:841–843.

Fukui, Y., T. J. Lynch, H. Brzeska, and E. D. Korn. 1989. Myosin I is located at the leading edges of locomoting Dictyostelium amoebae. *Nature (Lond.).* 341:328–331.

Gadasi, H., and E. D. Korn. 1980. Evidence for differential intracellular localization of the Acanthamoeba myosin isoenzymes. *Nature (Lond.).* 286: 452–456.

Green, N., H. Alexander, A. Olson, S. Alexander, T. M. Shinnick, J. G. Sutcliffe, and R. A. Lerner. 1982. Immunogenic structure of the influenza virus hemagglutinin. *Cell.* 28:477–487.

Halsall, D. J., and J. A. Hammer III. 1990. A second isoform of chicken brush border myosin I contains a 29-residue inserted sequence that binds to calmodulin. *FEBS (Fed. Eur. Biochem. Soc.) Lett.* 267:126–130.

Hayden, S. M., J. S. Wolenski, and M. S. Mooseker. 1990. Binding of brush border myosin I to phospholipid vesicles. *J. Cell Biol.* 111:443–451.

Henikoff, S. 1987. Unidirectional digestion with exonuclease III in DNA sequence analysis. *Methods Enzymol.* 155:156–165.

Hulen, D., A. Baron, J. Salisbury, and M. Clarke. 1991. Production and specificity of monoclonal antibodies against calmodulin from Dictyostelium discoideum. *Cell Motil. Cyutoskel.* 18:113–122.

Jung, G., and J. A. Hammer III. 1990. Generation and characterization of Dictyostelium cells deficient in a myosin I heavy chain isoform. *J. Cell Biol.* 110:1955–1964.

Jung, G., and J. A. Hammer III. 1994. The actin binding site in the tail domain of Dictyostelium myosin IC (myoC) resides within the glycine- and proline-rich sequence (tail homology region 2). *FEBS (Fed. Eur. Biochem. Soc.) Lett.* 342:197–202.

Jung, G., E. D. Korn, and J. A. Hammer III. 1987. The heavy chain of Acanthamoeba myosin IB is a fusion of myosin-like and non-myosin-like sequences. *Proc. Natl. Acad. Sci. USA.* 84:6720–6724.

Jung, G., C. L. Saxe III, A. R. Kimmel, and J. A. Hammer III. 1989*a*. Dictyostelium discoideum contains a gene encoding a myosin I heavy chain. *Proc. Natl. Acad. Sci. USA.* 86:6186–6190.

Jung, G., C. J. Schmidt, and J. A. Hammer III. 1989*b*. Myosin I heavy chain genes of Acanthamoeba castellanii: cloning of a second gene and evidence for the existence of a third isoform. *Gene.* 82:269–280.

Jung, G., Y. Fukui, B. Martin, and J. A. Hammer III. 1993. Sequence, expression pattern, intracellular localization, and targeted disruption of the Dictyostelium myosin ID heavy chain isoform. *J. Biol. Chem.* 268:14981–14990.

Kitamura, D., H. Kaneko, Y. Miyagoe, T. Ariyasu, and T. Watanabe. 1989. Isolation and characterization of a novel human gene expressed specifically in the cells of hematopoetic lineage. *Nucleic Acids Res.* 17:9367–9369.

Kozak, M. 1991. An analysis of vertebrate mRNA sequences: intimations of translational control. *J. Cell Biol.* 115:887–903.

Laemmli, U. K. 1970. Cleavage of structural proteins during assembly of the head of bacteriophage T4. *Nature (Lond.).* 227:680–685.

Lowenstein, E. J., R. J. Daly, W. Li, A. G. Batzer, B. Margolis, R. Lammers, A. Ullrich, E. Skolnik, D. Bar-Sagi, and J. Schlessinger. 1992. The SH2 and SH3 domain-containing protein GRB2 links receptor tyrosine kinases to ras signaling. *Cell.* 70:431–442.

Lynch, T. J., H. Brzeska, H. Miyata, and E. D. Korn. 1989. Purification and characterization of a third isoform of myosin I from Acanthamoeba castellanii. *J. Biol. Chem.* 264:19333–19339.

Maruta, H., and E. D. Korn. 1977. Acanthamoeba cofactor protein is a heavy-chain kinase required for actin activation of Mg^{2+}-ATPase activity of Acanthamoeba myosin I. *J. Biol. Chem.* 252:8329–8332.

Maruta, H., H. Gadasi, J. H. Collins, and E. D. Korn. 1978. The isolated heavy chain of an Acanthamoeba myosin contains full enzymatic activity. *J. Biol. Chem.* 253:6297–6300.

Matuoka, K., A. Yamakawa, M. Shibata, and T. Takenawa. 1992. Cloning of ASH, a ubiquitous protein composed of one Src homology region (SH) 2 and two SH3 domains, from human and rat cDNA libraries. *Proc. Natl. Acad. Sci. USA.* 89:9015–9019.

Meriläinen, J., R. Palovuori, R. Sormunen, V.-M. Wasenius, and V.-P. Lehto. 1993. Binding of the α-fodrin SH3 domain to the leading lamellae of locomoting chicken fibroblasts. *J. Cell Sci.* 105:647–654.

Miyata, H., B. Bowers, and E. D. Korn. 1989. Plasma membrane association

of *Acanthamoeba* myosin I. *J. Cell Biol.* 109:1519–1528.
Molina, M. I., K. E. Kropp, J. Gulick, and J. Robbins. 1987. The sequence of an embryonic myosin heavy chain gene and isolation of its corresponding cDNA. *J. Biol. Chem.* 262:6478–6488.
Murphy, S. M., M. Bergman, and D. O. Morgan. 1993. Suppression of c-src activity by C-terminal src-kinase involves the c-src SH2 and SH3 domains: analysis with Saccharomyces cerevisiae. *Mol. Cell. Biol.* 13:5290–5300.
Okada, M., B. W. Howell, M. A. Broome, and J. A. Cooper. 1993. Deletion of the SH3 domain of src interferes with regulation by the phosphorylated carboxyl-terminal tyrosine. *J. Biol. Chem.* 268:18070–18075.
Pawson, T., and J. Schlessinger. 1992. SH2 and SH3 domains. *Curr. Biol.* 3:434–442.
Pollard, T. D., S. K. Doberstein, and H. G. Zot. 1991. Myosin-I. *Annu. Rev. Physiol.* 53:653–681.
Rayment, I., W. R. Rypniewski, K. Schmidt-Bäse, R. Smith, D. R. Tomchick, M. M. Benning, D. A. Winkelmann, G. Wesenberg, and H. M. Holden. 1993. Three-dimensional structure of myosin subfragment-1: a molecular motor. *Science (Wash. DC).* 261:50–58.
Ren, R., B. J. Mayer, P. Cicchetti, and D. Baltimore. 1993. Identification of a ten-amino acid proline-rich SH3 binding site. *Science (Wash. DC).* 259:1157–1161.
Rosenfeld, S. S., and B. Rener. 1994. The GPQ-rich segment of Dictyostelium myosin IB contains an actin binding site. *Biochemistry.* 33:2322–2328.
Ruppert, C., R. Kroschewski, and M. Bähler. 1993. Identification, characterization and cloning of myr 1, a mammalian myosin-I. *J. Cell Biol.* 120: 1393–1403.
Sanger, F., S. Nicklen, and A. Coulson. 1977. DNA sequencing with chain terminating inhibitors. *Proc. Natl. Acad. Sci. USA.* 74:5463–5467.
Schröder, R. R., D. J. Manstein, W. Jahn, H. Holden, I. Rayment, K. C. Holmes, and J. A. Spudich. 1993. Three-dimensional atomic model of F-actin decorated with Dictyostelium myosin S1. *Nature (Lond.).* 364: 171–174.
Slaughter, G. R., and A. R. Means. 1987. Use of the ^{125}I- labeled protein gel overlay technique to study calmodulin-binding proteins. *Methods Enzymol.* 139:433–444.
Superti-Furga, G., S. Fumagalli, M. Koegl, S. A. Courtneidge, and G. Draetta. 1993. Csk inhibition of c-src activity requires both the SH2 and SH3 domains of src. *EMBO (Eur. Mol. Biol. Org.) J.* 12:2625–2634.
Titus, M. A., D. Wessels, J. A. Spudich, and D. Soll. 1993. The unconventional myosin encoded by the myoA gene plays a role in Dictyostelium motility. *Mol. Biol. Cell.* 4:233–246.
Towbin, H., T. Staehelin, and J. Gordon. 1979. Electrophoretic transfer of proteins from polyacrylamide gels to nitrocellulose sheets: procedure and some applications. *Proc. Natl. Acad. Sci. USA.* 76:4350–4354.
Toyoshima, Y. Y., S. J. Kron, E. M. McNally, K. R. Niebling, C. Toyoshima, and J. A. Spudich. 1987. Myosin subfragment-1 is sufficient to move actin in vitro. *Nature (Lond.).* 328:536–539.
Wessels, D., J. Murray, G. Jung, J. A. Hammer III, and D. R. Soll. 1991. Myosin IB null mutants of Dictyostelium exhibit abnormalities in motility. *Cell Motil. Cytoskel.* 20:301–315.
Wu, H., A. B. Reynolds, S. B. Kanner, R. R. Vines, and J. T. Parsons. 1991. Identification and characterization of a novel cytoskeleton-associated pp60^{src} substrate. *Mol. Cell. Biol.* 11:5113–5124.
Yonemura, S., and T. D. Pollard. 1992. The localization of myosin I and myosin II in Acanthamoeba by fluorescence microscopy. *J. Cell Sci.* 102:629–642.